

Supporting Information

For

Facile synthesis of Cu-based catalysts from Cu₃Si and their catalysis properties study

Yonghui Li¹, Xianhui Liu¹, Guangfu Zu¹, Zhiwei Yang², Xiao Huang², Shaozhou Li^{1}*

1. State Key Laboratory of Organic Electronics and Information Displays & Institute of Advanced Materials, Nanjing University of Posts & Telecommunications, 9 Wenyuan Road, Nanjing 210023, China

2. Key Laboratory of Flexible Electronics (KLOFE) & Institute of Advanced Materials (IAM), Jiangsu National Synergistic Innovation Center for Advanced Materials (SICAM), Nanjing Tech University (NanjingTech), 30 South Puzhu Road, Nanjing 211816, China.

E-mail: iamszli@njupt.edu.cn.

Experimental Section

Synthesis of Cu₃Si@Si: In a typical synthesis procedure, 1 g of silicon particles with different sizes and 2 g of anhydrous cuprous chloride were placed in a mortar to ground and mix. The mixture was then transferred to an alumina boat and heated in a tube furnace under N₂ condition at 800°C for 1 hour. After natural cooling to room temperature, a brown-black powder was obtained.

Synthesis of CuSiO₃@SiO_x: 0.6 g of Cu₃Si@Si powder obtained was dispersed in a mixture solution of 20 ml ultrapure water and 10 ml ammonia solution (25%~28%) and stirred magnetically for 5 min at room temperature. The solution was then transferred to an autoclave and heated at 120°C in oven for 24 hours. Subsequently, it was centrifuged and washed with water and ethanol. Finally, the product was vacuum dried at 80°C for 12 hours to obtain the copper silicate samples.

Synthesis of Cu@SiO_x/Si: 20 ml of KCl solution (4 M) was mixed with 10 ml of ammonia solution (25%~28%). Next, 0.6 g of Cu₃Si@Si powder was dispersed in the mixed solution and stirred magnetically for 5 min at room temperature. The mixture solution was then transferred to an autoclave and heated at 120°C in oven for 24 hours. Subsequently, it was centrifuged and washed with water and ethanol. Finally, the product was vacuum dried at 60°C for 12 hours to obtain the Cu@SiO_x/Si.

Characterizations: X-ray diffraction (XRD, SmartLab Rigaku) was performed with Cu K α radiation ($\lambda=1.54 \text{ \AA}$) as the X-ray source. The UV-vis-NIR absorption spectrum was recorded by LAMBDA 650S. Scanning electron microscopy (SEM, Hitachi S-4800) was used for the morphology analysis. To gain the crystal structure information, high-resolution transmission electron microscopy (HRTEM, JEOL 2100F) coupled with energy dispersive X-ray (EDX) spectroscopy analyses were performed. N₂ adsorption isotherms were measured by the Brunauer-Emmett-Teller (BET, Micrometrics ASAP2460) method, and the samples were pretreated at 150 °C in vacuum overnight. The chemical state study of the samples was carried out by XPS (PHI 5000 VersaProbe) and the binding energies were corrected for specimen charging effects using the C 1s level at 284.6 eV as the reference.

4-nitrophenol reduction: 0.1 ml of a 4-nitrophenol (p-NP) solution (0.16 mol/L) was mixed with 1 ml of a NaBH₄ solution (0.26 mol/L, prepared using an ice-water mixed solvent) and 15 ml of deionized water in a test tube. Subsequently, 2 mg of catalyst was added into the solution then, and the reaction was carried out at room temperature. The change in the absorption peak of the nitrophenol ions at a wavelength of 400 nm was recorded every 40 seconds using a UV-visible spectrophotometer. After the reaction, the catalyst was collected via a high-speed centrifugation method and reintroduced into the same concentration of reaction solution to test the efficiency of catalyst reusability. This process is repeated five times to assess the recyclability and reusability performance of the catalyst. The kinetic analysis of the catalytic

reduction reactions was characterized by the attenuation intensity of peaks over different time intervals. Given that the concentration of NaBH₄ is significantly higher than that of 4-NP, the reaction kinetics constant and rate are independent of the NaBH₄ concentration. Therefore, the reaction rate constants can be evaluated using pseudo-first-order kinetics, as demonstrated in the following equation:

$$\frac{dC_t}{dt} = -k_{app}C_t \quad (1)$$

$$\ln\left(\frac{C_t}{C_0}\right) = \ln\left(\frac{A_t}{A_0}\right) = -k_{app}t \quad (2)$$

where C_t and A_t represent the concentration and absorbance of p-NP at time t, respectively, C₀ and A₀ denote the initial concentration and absorbance of p-NP at t=0. The term k_{app} refers to the apparent rate constant.

The cycling stability is characterized by the conversion efficiency after cycling, as demonstrated in the following equation:

$$D = \frac{C_0 - C_t}{C_0} \times 100\% = \frac{A_0 - A_t}{A_0} \times 100\% \quad (3)$$

To diminish the effect of the loss of catalyst during centrifugation, the amount of catalyst is increased from 2 mg to 8 mg.

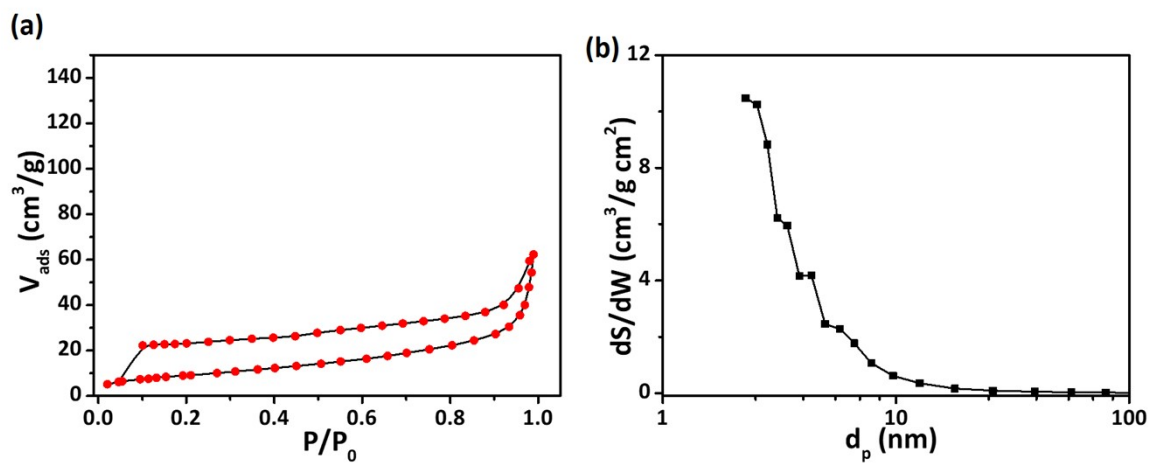


Figure S1. (a) Nitrogen adsorption-desorption isotherms of Cu@SiO_x/Si nanoparticles. (b) The pore size distribution calculated based on the NLDFT model.

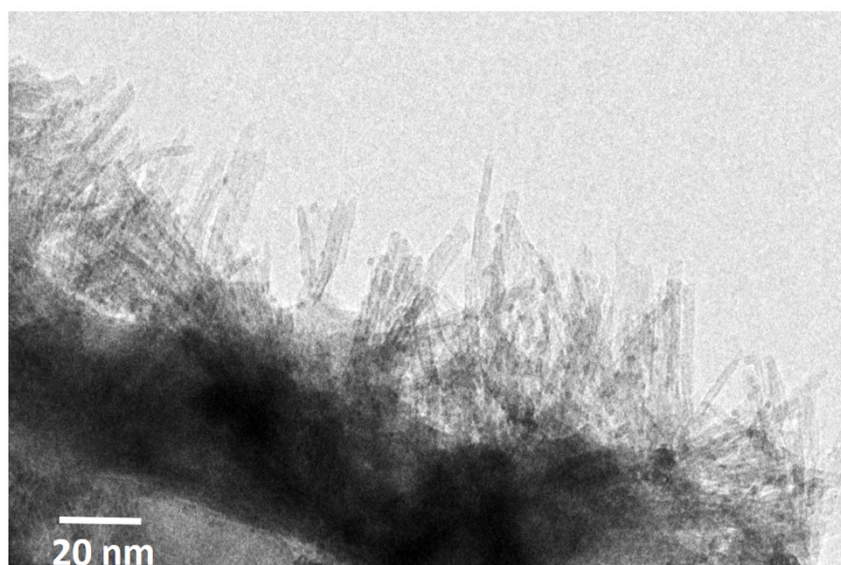


Figure S2. TEM image of NaBH₄ reduced CuSiO₃@SiO_x nanoparticles. The small dark spots are reduced Cu nanoparticles.

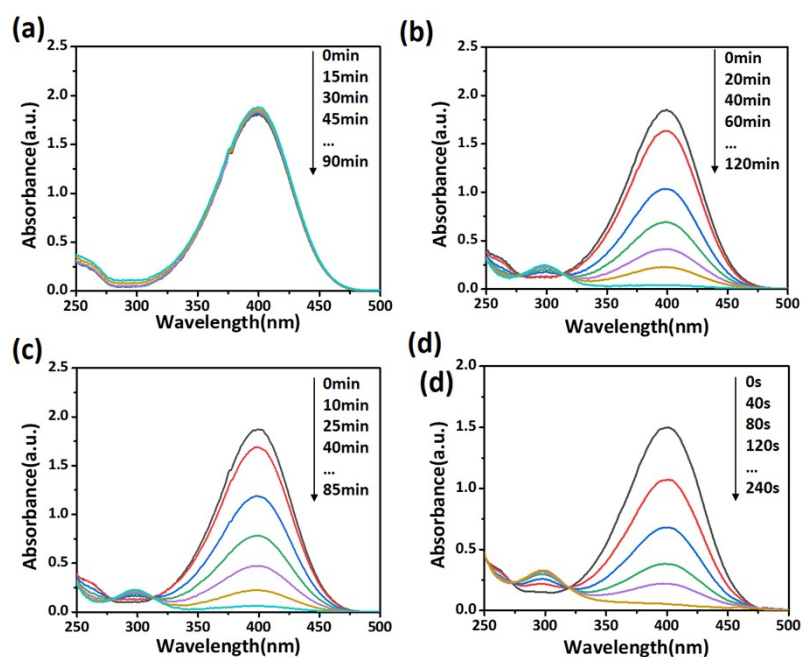


Figure S3. (a) UV-vis spectra for the catalytic reduction of 4-NP using Si NPs as catalyst. (b) UV-vis spectra for the catalytic reduction of 4-NP using $\text{CuSiO}_3@\text{SiO}_x$ NPs as catalyst. (c) UV-vis spectra for the catalytic reduction of 4-NP using the NaBH_4 reduced $\text{CuSiO}_3@\text{SiO}_x$ NPs as catalyst. (d) UV-vis spectra for the catalytic reduction of 4-NP using $\text{Cu}@\text{SiO}_x/\text{Si}$ NPs as catalyst.

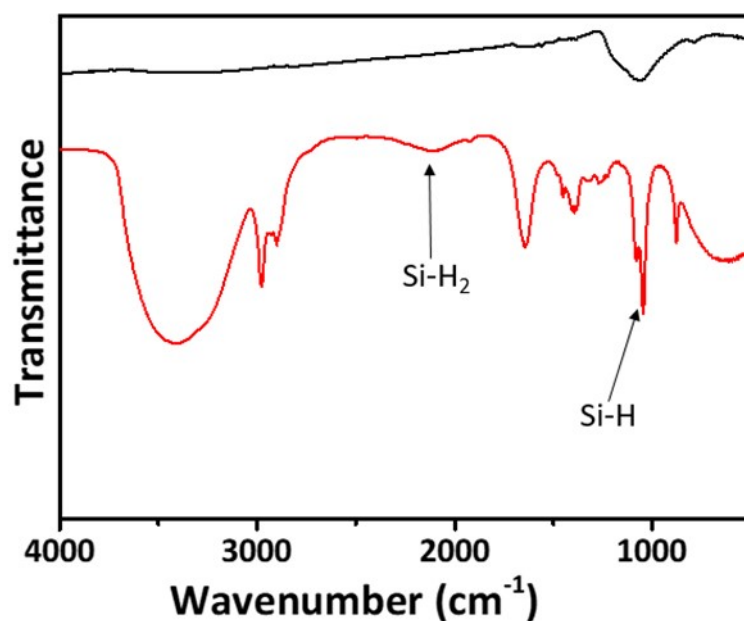


Figure S4. FTIR spectra of $\text{Cu}@\text{SiO}_x/\text{Si}$ before and after catalytic reaction.

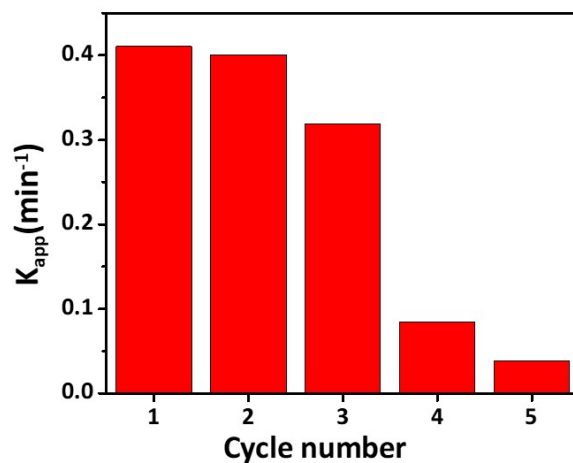


Figure S5. Reusability of the Cu@SiO_x/Si catalyst upon repeated application for the catalytic reduction of 4-NP in which 2 mg catalyst is used. The dramatic decrease of its catalytic performance is more likely attributed to the loss and aggregation of Cu@SiO_x/Si during centrifugation.

Table S1. Comparison of 4-NP reduction by various metal NPs and their bimetallic catalysts from the literature

Metallic NP	Support [Ref.]	K_{app} [min ⁻¹]	C(4-NP),mmol/L	C(NaBH ₄),mmol/L	C(catalyst),mg/L	Reaction time/min	Reference
RuNPs	CS-CR@Mn	4.68	16.6	50.0	333.3	1	1
	HHP	0.36	0.09	9.9	123.8	5	2
CoNPs	NCNTS	0.37	0.21	38.5	30.7	6	3
	HNTs-ILs	0.60	2.87	270.2	1000	13	4
ZnNPs	SnO ₂	0.59	0.07	3.11	505.5	22	5
	C	1.17	0.19	48.1	19.2	2.5	6
NiNPs	CuS	1.06	0.10	10.0	500	4	7
	SiO ₂	0.27	0.16	64	967.7	10	8
	Mn ₂ O ₃	0.13	0.10	60	400	45	9
	APTES@Fe ₃ O ₄	0.27	0.17	67	9.92	10	10
CuNPs	RGO	0.35	0.15	14.4	9.63	10	11
	MnO ₂	0.68	0.10	20.6	6.66	6	12
	AG-sponge	0.32	0.13	28.6	5714.2	11	13
	N-doped carbon	1.78	0.10	10.3	44.4	11	14
	Cs@CMC	0.38	0.13	66.6	166.6	7	15
	Mag-S-Ms	0.24	0.05	4	333.3	10	16
	g-C ₃ N ₄	1.11	0.13	13.70	17.24	6	17
	zeolite	0.21	0.2	15	250	3.5	18
	SiOx@Si	0.40	0.10	3.29	120	4	This work
	g-C ₃ N ₄	0.23	0.11	5.89	98.10	14	19
AgNPs	ZrGP	0.18	0.09	45.4	90.90	10	20
	SrTiO ₃	0.54	0.30	20	200	7	21
	HCP-BHMB-K-800	1.26	0.09	22.7	22.72	2.5	22
	PVP-PS	0.10	0.14	14.5	388.3	60	23
PdNPs	Azo-POPs	0.34	0.12	5.12	2.5	10	24
	CeO ₂	0.46	0.06	31.3	-	6.7	25
	Co-MOF	0.25	0.10	30.0	0.75	8	26

- 1 K. H. Liew, T. K. Lee, M. A. Yarmo, K. S. Loh, A. F. Peixoto, C. Freire and R. M. Yusop, *Catalysts*, 2019, **9**, 254.
- 2 M. Gopiraman, S. Saravanamoorthy and I.-M. Chung, *Res. Chem. Intermed.*, 2017, **43**, 5601-5614.
- 3 X. Wang, G. Si, Y. Kou, M. Ding, S. Zhang, J. Huang and X. Xu, *J. Alloys Compd.*, 2021, **858**, 158287.
- 4 K. Yavari, B. Eftekhari-Sis and A. Akbari, *NANO*, 2021, **16**, 2150089.
- 5 S. K. Jain, U. Farooq, F. Jamal, A. Kalam and T. Ahmad, *Mater. Today: Proc.*, 2021, **36**, 717-723.
- 6 J. Rong, F. Qiu, T. Zhang, Y. Zhu, J. Xu, Q. Guo and X. Peng, *Appl. Surf. Sci.*, 2018, **447**, 222-234.
- 7 Y.-R. MA, W. ZHOU, W. CAO, J.-L. ZHENG and L. GUO, *Acta Phys. Chim. Sin.*, 2015, **31**, 1949-1955.
- 8 Z. Niu, S. Zhang, Y. Sun, S. Gai, F. He, Y. Dai, L. Li and P. Yang, *Dalton Trans.*, 2014, **43**, 16911-16918.
- 9 P. Deka, P. Sarmah, R. C. Deka and P. Bharali, *ChemistrySelect*, 2016, **1**, 4726-4735.
- 10 Y. Zhong, Y. Gu, L. Yu, G. Cheng, X. Yang, M. Sun and B. He, *Colloids Surf., A*, 2018, **547**, 28-36.
- 11 L. Qin, H. Xu, K. Zhu, S.-Z. Kang, G. Li and X. Li, *Catal. Lett.*, 2017, **147**, 1315-1321.
- 12 C. Du, S. He, X. Gao and W. Chen, *ChemCatChem*, 2016, **8**, 2885-2889.
- 13 T. Kamal, A. M. Asiri and N. Ali, *Spectrochim. Acta, Part A*, 2021, **261**, 120019.
- 14 P. Li, H. Wang, S. Jiang, J. Wang, Z. Cao and J. Yang, *Applied Catalysis A: General*, 2022, **631**, 118479.
- 15 N. Maslamani, S. B. Khan, E. Y. Danish, E. M. Bakhsh, K. Akhtar and A. M. Asiri, *Chemosphere*, 2022, **291**, 133010.
- 16 Y. Yu, H. Guo, P. Wang, S. Zhai, J. Han, W. Li, Y. Wang and Y. Wang, *Res. Chem. Intermed.*, 2023, **49**, 381-397.
- 17 S. Huang, Y. Zhao and R. Tang, *RSC Adv.*, 2016, **6**, 90887-90896.
- 18 A. H. Zahmani, R. M. Kerbadou, A. Benmaati, M. Hachemaoui, I. Issam, J. Iqbal, S. Hacini, B. Boukoussa and H. H. Zahmani, *Inorg. Chem. Commun.*, 2023, **156**, 111211.
- 19 X. Wang, F. Tan, W. Wang, X. Qiao, X. Qiu and J. Chen, *Chemosphere*, 2017, **172**, 147-154.
- 20 A. Zhou, J. Li, G. Wang and Q. Xu, *Appl. Surf. Sci.*, 2020, **506**, 144570.
- 21 Z. Wu, Y. Zhang, X. Wang and Z. Zou, *New J. Chem.*, 2017, **41**, 5678-5687.
- 22 K. Zhang, Q. Wang, Z. Zhong, Y. Luo, J. Liu, Y. Liu and Y. Lyu, *New J. Chem.*, 2024, **48**, 2321-2326.
- 23 B. Lakshminarayana, K. A. Kumar, M. Selvaraj, G. Satyanarayana and S. Ch, *J. Environ. Chem. Eng.*, 2020, **8**, 103899.
- 24 Y. Yu, Y. Gong, B. Cao, H. Liu, X. Zhang, X. Han, S. Lu, X. Cao and H. Gu, *Chem. Asian J.*, 2021, **16**, 837-844.
- 25 W. Wang, G. Dai, H. Yang, X. Liu, X. Chen, Z. Meng and Q. He, *Environ. Sci. Pollut. Res.*, 2022, **29**, 8242-8252.
- 26 X. Duan, A. Liu, L. Zhou and S. Wei, *Environ. Sci. Pollut. Res.*, 2023, **30**, 97936-97947.